International Journal of Scientific Research in Engineering and Management (IJSREM)
Volume: 10 Issue: 10 | Oct - 2026 SJIF Rating: 8.659 ISSN: 2582-3930

Design and Kinematic Analysis of a High-Speed Mechanical Hammering Machine Using a Cycloidal Cam Mechanism

Deep Kalsariya[1], Siddharth Parmar[2], Karan Rakholiya[3], Yogesh Dholariya[4]

[1, 2, 3]UG Students, Department of Mechanical Engineering, SoET, Dr. Subhash University, Junagadh, Gujarat, India
[4]Assistant Professor, Department of Mechanical Engineering, SoET, Dr. Subhash University, Junagadh, Gujarat, India.

E-mail: kalsariyadeep11@gmail.com, sidparmar987@gmail.com, karanrakholiya775@gmail.com, yogeshraj2202@gmail.com

Abstract - Many mechanical hammering machines are driven by crank or eccentric mechanisms, which give the hammer a near-sinusoidal stroke that spends as long going down as coming up. This paper examines a cam-driven alternative in which a single-lobe disc cam with a roller follower gives the hammer a cycloidal downstroke over only 99° of cam rotation and a 180° return. A 1 HP, 1440 rpm motor and a three-stage V-belt reduction (14.06:1) set the camshaft at 102.4 rpm, so each blow takes 0.586 s and the descent lasts 161 ms. For a 97.8 mm follower stroke and a 99.7 mm hammer stroke, cycloidal kinematics give a peak hammer velocity of 1.24 m/s, a peak acceleration of 24.1 m/s² and 1.53 J of kinetic energy for a 2 kg hammer. At the same stroke and shaft speed this is 3.3 times the energy of a symmetric cycloidal profile and 5.4 times that of simple harmonic motion, but the peak lever load rises from 34 N to 68 N and the pressure angle reaches about 34°. All results are analytical; no impact measurements are reported.

Keywords: Cam-follower mechanism, cycloidal motion, mechanical hammer, belt-pulley reduction, impact energy, kinematic analysis.

1. INTRODUCTION

A hammering machine shapes metal by delivering a short, hard blow and the result depends largely on the kinetic energy the hammer carries when it meets the work. For a hammer of mass m moving at velocity v, that energy is $E_k = \frac{1}{2}mv^2$, so velocity counts twice as heavily as mass. Neither can be raised freely. A heavier hammer loads the lever, bearings and frame in proportion to its weight and a faster-running drive raises inertial loads with the square of shaft speed.

Hammering machines come in several forms. Gravity-drop and pneumatic hammers can deliver heavy blows, but the velocity profile and timing of each blow are hard to control precisely. Mechanical hammers, driven by a motor through belts and a motion-conversion mechanism, are simpler to build and keep running and most of them use a crank, an eccentric or a four-bar linkage. To a first approximation these give a symmetric, sinusoidal stroke in which the hammer takes about as long to come down as it does to go back up. If the hammer must travel a fixed distance in half a revolution, its velocity is capped by the shaft speed and the only ways to raise it are to run the shaft faster or to add mass.

A cam removes that restriction. Its profile can assign any share of a revolution to the downstroke, the return and the dwells and the follower reproduces whatever motion law the designer prescribes. If the downstroke is compressed into a smaller cam angle and the return takes the rest, the hammer covers the same stroke in less time, so its velocity rises without any change in shaft speed or hammer mass. The price is a steeper acceleration, because the same distance must be covered faster and then stopped. Cycloidal motion suits this job: velocity and acceleration are both zero at the start and end of the rise, so the follower enters and leaves its dwell positions without a sudden change of acceleration.

This paper studies a hammering machine built on that idea. A 1 HP motor drives a three-stage V-belt reduction to a camshaft turning at 102.4 rpm. A single-lobe disc cam with a roller follower assigns 99° to the downstroke, 15° to a dwell at the bottom, 180° to the return and 66° to a dwell at the top and an existing lever and hammer assembly carries the motion to a 2 kg hammer. A prototype has been fabricated, but the work reported here is analytical. No impact measurements have been made and every number below comes from calculation.

The paper does three things. It lays out the design calculations from motor to hammer as one consistent chain. It computes the cycloidal kinematics directly from the governing equations. And it compares the 99° downstroke with symmetric alternatives at equal stroke and shaft speed, so that the gain in impact energy and the cost in lever load can be read from the same model. Section II reviews related work, Section III describes the method, Section IV gives the results, Section V interprets them and Section VI closes with limitations and takeaways.

2. LITERATURE REVIEW

A. Power Hammers and Impact Energy

Published work on small power hammers is mostly design-and-build reporting. Al Aamri et al. modelled a compact, low-cost power hammer in AutoCAD and sized it from kinetic principles, calculating motor capacity, impact velocity, torque and kinetic energy before fabrication [1]. That is the sensible way to size a machine and the calculation sequence used in this paper follows the same logic. In an approach of this kind, however, impact velocity is an output of whichever drive was chosen. It is not a quantity the drive is shaped to deliver.

B. Cam-Follower Motion Design

The classical motion laws (constant acceleration, simple harmonic, cycloidal and polynomial) and the geometric relations for cams with roller followers are standard textbook material [2, 3]. Recent research has moved mostly towards spline-based descriptions. Qiu et al. represented cam curves with uniform B-splines and optimised them against kinematic and dynamic objectives, including residual vibration in an indexing mechanism [4]. Nguyen et al. proposed a general framework for follower motion design based on NURBS [5] and Mandal and Naskar examined how adding control points changes a spline-based motion programme [6]. On the dynamic side, Gatti and Mundo addressed follower vibration directly [7], Desai and Patel developed a computer-aided kinematic and dynamic analysis of a cam

and follower [8] and Wu et al. designed varying-velocity translating cam mechanisms [9]. For sizing, Avelar and Soares published nomograms for the maximum pressure angle of radial cams with follower eccentricity under cycloidal and harmonic motion and they state the empirical limit of 30° that radial cams with translating roller followers are normally held to [10].

C. Belt Drives

For the transmission, the working references are the machine-design text of Khurmi and Gupta and the handbook of belt-drive principles and calculations by Perneder and Osborne [11,12], which give belt geometry, tension relations and power capacity. Research on belt drives is mostly concerned with dynamic effects. Pellicano et al. studied parametric instability of belts, with theory and experiments [13]; Čepon and Boltežar modelled belt-pulley contact in a belt-drive system [14]; Chowdhury and Yedavalli analysed the dynamics of belt-pulley-shaft systems [15]; and Bertini et al. built an analytical model of power losses in a rubber V-belt drive [16].

D. Gap Addressed Here

Read together, these studies are largely about making cam motion smoother, reducing vibration, lowering contact stress or accounting for belt losses, usually at the speeds of valve trains, indexing machines and automotive drives. None of the work reviewed here asks the question a hammer designer asks: how much impact energy is gained by squeezing the downstroke into a small part of the cam cycle and what does that cost in acceleration, lever load and pressure angle? The classical cycloidal law has closed-form equations and is sufficient to answer it, which is why it is used here instead of a spline.

3. METHODOLOGY

A. Machine Layout and Design Sequence

Fig. 1 shows the machine and the numbers in this paragraph refer to it. A single-phase 1 HP induction motor (1) running at 1440 rpm drives three V-belt stages in series (2). The last shaft carries a 180 mm pulley and the cam (3). A roller follower of 15 mm radius rides on the cam and a compression spring between the follower and the connecting link (4) keeps the two in contact. The link (5), a 20 × 20 mm bar about 890 mm long, carries the follower motion to the leaf-spring lever (6), which pivots on a fixed fulcrum (7). Because the fulcrum lies between the link and the hammer rod, the lever reverses the direction of travel and cam rise becomes hammer descent. The leaf spring also gives the lever a little elastic compliance. The hammer (8) is a hollow cylindrical head, 127 mm in outside diameter and 40 mm high, on a 50 × 50 mm square rod 550 mm long and the moving assembly is taken as 2 kg. The work rests on the anvil (9). The frame, rod, cam and fulcrum are mild steel and the pulleys are cast iron.

The initial design basis, listed in Table I, was a 2 kg hammer with a working stroke of about 100 mm, a faster downstroke and a controlled return, produced by a cycloidal cam with a roller follower. The cam is driven through three belt stages by a single-phase induction motor that runs continuously, because the machine is meant to operate under repeated impact for long periods.

TABLE I. DESIGN REQUIREMENTS

Requirement	Specification
Hammer mass	2 kg
Working stroke	about 100 mm
Downstroke	higher velocity
Return stroke	controlled upward motion
Motion generation	cycloidal cam, roller follower
Power transmission	belts and pulleys, three stages
Motor	single-phase induction, continuous duty
Operation	repeated impact, continuous running

The design followed a fixed order. The camshaft speed and cam timing were settled first (Section III-C). The belt drive was then divided into stages to reach that speed (Section III-B), the cycloidal kinematics of the follower were derived (Section III-D) and the lever ratio was used to turn follower motion into hammer velocity, load and energy (Section III-E). Finally, the result was compared with alternative motion laws and checked for pressure angle and power (Section III-F). Throughout, links are treated as rigid, belts as slip-free and friction as negligible, so every figure is an ideal value and measured performance will differ.

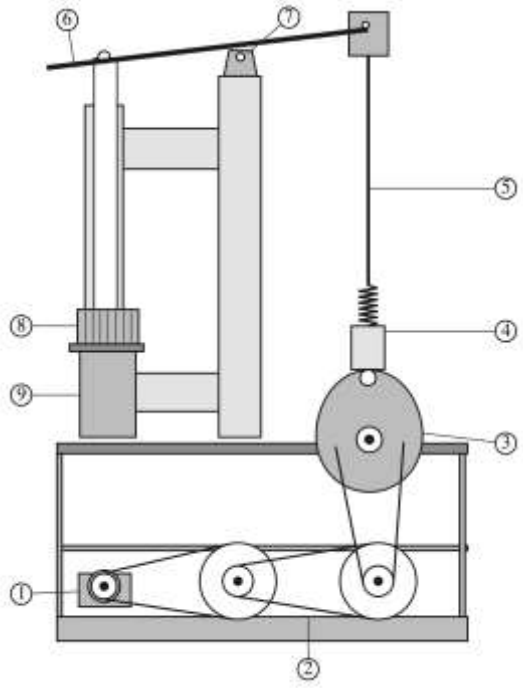


Fig. 1. Schematic front view of the machine, redrawn from the CAD model and not to scale: (1) motor, (2) three-stage belt-pulley drive, (3) cam, (4) roller follower with compression spring, (5) connecting link, (6) leaf-spring lever, (7) fulcrum, (8) hammer rod and head, (9) anvil.

B. Drive and Speed Reduction

The overall reduction i_o and the camshaft speed N_c follow from the three stage ratios, each being the driven-to-driver pulley diameter ratio:

$$i_o = i_1\, i_2\, i_3, \qquad N_c = \frac{N_m}{i_o} \tag{1}$$

The motor torque at rated power P_m and speed N_m is

$$T_m = \frac{60\, P_m}{2\pi N_m} \tag{2}$$

and the ideal torque on the k-th shaft, before any losses, is

$$T_k = T_m\, i_1\, i_2 \cdots i_k \tag{3}$$

For an open belt drive with driver diameter D_1, driven diameter D_2 and centre distance C, the wrap angle on the small pulley is

$$\theta_w = \pi - 2\sin^{-1}\left(\frac{D_2 - D_1}{2C}\right) \quad (4)$$

and the belt length is

$$L_b = 2C + \frac{\pi(D_1 + D_2)}{2} + \frac{(D_2 - D_1)^2}{4C} \quad (5)$$

The belt speed and the tension difference needed to carry the motor power through n_b belts, are

$$v_b = \frac{\pi D_1 N_1}{60}, \qquad T_1 - T_2 = \frac{P_m}{n_b\, v_b} \quad (6)$$

where N_1 is the driver speed in rpm [11], [12]. The first stage sees the highest belt speed and was checked in detail. The second and third stages use the same B-section belt family.

C. Cam Motion Programme and Timing

One cam revolution produces one blow. The camshaft angular velocity and the cycle time are

$$\omega_c = \frac{2\pi N_c}{60}, \qquad \tau = \frac{60}{N_c} \quad (7)$$

and a motion occupying a cam angle β_i lasts

$$t_i = \frac{\beta_i}{360}\,\tau \quad (8)$$

The cam angle is divided as follows: a 99° rise, during which the hammer descends; a 15° dwell at the bottom; a 180° return, during which the hammer rises; and a 66° dwell at the top, which completes the 360°. The downstroke is deliberately given the smallest angle, because a short descent time is what raises velocity at a fixed stroke. The value of 99° is a design choice and not a derived optimum and Section V discusses how the results scale with it.

D. Cycloidal Follower Kinematics

For a follower that rises through a stroke h over a cam angle β, the cycloidal law gives displacement, velocity and acceleration in terms of the cam angle θ, measured from the start of the rise [2], [3]:

$$s_f(\theta) = h\left[\frac{\theta}{\beta} - \frac{1}{2\pi}\sin\left(\frac{2\pi\theta}{\beta}\right)\right] \quad (9)$$

$$v_f(\theta) = \frac{h\,\omega_c}{\beta}\left[1 - \cos\left(\frac{2\pi\theta}{\beta}\right)\right] \quad (10)$$

$$a_f(\theta) = \frac{2\pi h\,\omega_c^2}{\beta^2}\sin\left(\frac{2\pi\theta}{\beta}\right) \quad (11)$$

Velocity peaks at $\theta = \beta/2$ and acceleration at $\theta = \beta/4$ and $3\beta/4$, with peak values

$$v_{f,\max} = \frac{2h\,\omega_c}{\beta}, \qquad a_{f,\max} = \frac{2\pi h\,\omega_c^2}{\beta^2} \quad (12)$$

The return stroke follows the same law with $\beta = 180°$. Two properties matter for what follows. The peak velocity is twice the mean velocity over the motion and the peaks scale as $1/\beta$ for velocity and $1/\beta^2$ for acceleration. Jerk stays finite, with a maximum of $4\pi^2 h\omega_c^3/\beta^3$ at the ends of the stroke. All values in this paper are computed from Eqs. (9)–(12) using h = 97.8 mm, the follower stroke given by the CAD model.

E. Lever Ratio, Hammer Load and Energy

The lever turns follower motion into hammer motion with a ratio equal to the hammer stroke S_h over the follower stroke:

$$i_L = \frac{S_h}{h} \quad (13)$$

Hammer velocity and acceleration scale by the same ratio:

$$v_h = i_L\, v_f, \qquad a_h = i_L\, a_f \quad (14)$$

The CAD model gives S_h = 99.7 mm for h = 97.8 mm, so i_L = 1.019. The preliminary lever arms, about 343 mm on the hammer side and 310 mm on the link side, would suggest 1.107, but the CAD model describes the motion more exactly and its ratio is used throughout. While the hammer is being slowed on its way down, the lever must push up on it with a force

$$F_{h,\max} = m_h\left(g + a_{h,\max}\right) \quad (15)$$

where m_h is the hammer mass and g = 9.81 m/s^2. The kinetic energy carried by the hammer at its peak velocity is

$$E_k = \frac{1}{2}\, m_h\, v_{h,\max}^2 \quad (16)$$

This is an upper bound on the energy the hammer can deliver. Whether all of it reaches the work depends on where the work surface sits, as Section V explains.

F. Comparison Cases and Checks

To judge what the 99° downstroke achieves, the same stroke, shaft speed and hammer mass were run through two reference motions: a symmetric cycloidal motion with a 180° descent and simple harmonic motion over 180°, which is the idealised behaviour of a crank. For simple harmonic motion the peak follower velocity is $\pi h\omega_c/(2\beta)$ and the peak acceleration is $\pi^2 h\omega_c^2/(2\beta^2)$, with $\beta = \pi$. A second comparison asks what it would take to reach the same energy by adding mass instead of shortening the descent. The mass needed at the symmetric cycloidal velocity is $m_{eq} = 2E_k/v_{h,sym}^2$ and the peak load follows from Eq. (15).

Two further checks were made. The pressure angle φ of an in-line (zero-offset) roller follower, which governs the sideways load on the follower guide, is

$$\tan\varphi = \frac{ds_f/d\theta}{R_p + s_f} \quad (17)$$

where $R_p = R_b + R_r$ is the prime-circle radius, R_b = 110 mm is the base-circle radius and R_r = 15 mm is the roller radius [2], [10]. It was evaluated over the whole rise and return. Finally, the power needed to lift the hammer was estimated as $m_h g S_h$ per cycle multiplied by the blow rate and compared with the motor rating.

G. Fabrication of the Prototype

The components were made to the CAD dimensions. Raw stock was measured and marked, cut with a hacksaw and the shafts were turned on a lathe, with stepped sections for the bearing and pulley seats. Holes were drilled where needed and the frame and supporting structure were welded. The frame was assembled first, followed by the shafts, pillow-block bearings, pulleys, belts, cam-follower mechanism and the lever and hammer. The follower and link were connected to the existing lever and the finished machine was checked for alignment, clearance and free movement. Performance measurements are not part of this study.

4. RESULTS

A. Transmission and Shaft Torque

Table II lists the three reduction stages. The 80/200, 80/200 and 80/180 mm pulley pairs give ratios of 2.5, 2.5 and 2.25, an overall reduction of 14.0625 and a camshaft speed of 102.4 rpm, which is ω_c = 10.72 rad/s. One cycle therefore lasts τ = 0.586 s and the hammer strikes 102.4 times a minute (1.71 Hz). The motor's rated torque is 4.95 N·m, so the ideal torque rises to 12.4, 30.9 and 69.6 N·m along the three shafts before losses.

TABLE II. THREE-STAGE V-BELT REDUCTION AND IDEAL SHAFT TORQUE

Stage	Pulleys D_1/D_2 (mm)	Ratio	Output speed (rpm)	Belts	Ideal torque (N·m)
Motor	–	–	1440	–	4.95
1	80/200	2.50	576.0	2 × B42	12.4
2	80/200	2.50	230.4	2 × B43	30.9
3	80/180	2.25	102.4	1 × B45	69.6
Overall	**–**	**14.06**	**102.4**	**–**	**–**

For the first stage (D_1 = 80 mm, D_2 = 200 mm, C = 342 mm), Eqs. (4)–(6) give a wrap angle of 159.8° (2.79 rad), a belt length of 1,134 mm and a belt speed of 6.03 m/s. The B42 belts selected, listed at 1,135 mm, agree with the computed length. With two belts sharing 746 W, each carries a tension difference of 61.8 N and the design tensions of T_1 = 67.7 N and T_2 = 5.86 N per belt reproduce it (61.84 N).

B. Cam Timing

Table III gives the cam timing. The downstroke takes 99° of rotation, 27.5% of the cycle and lasts 161 ms, while the return takes half the cycle (293 ms). The mean hammer speed is therefore 0.619 m/s going down and 0.340 m/s coming back, so even on average the downstroke is about 1.8 times faster than the return.

TABLE III. CAM TIMING OVER ONE REVOLUTION

Phase	Angle (°)	Follower motion	Time (ms)	Share (%)
Rise (down)	99	0 → 97.8 mm	161.1	27.5
Dwell, bottom	15	held	24.4	4.2
Return (up)	180	97.8 → 0 mm	293.0	50.0
Dwell, top	66	held	107.4	18.3
Total	**360**	**–**	**585.9**	**100.0**

C. Follower Kinematics

Table IV lists the 99° rise at 11° intervals and Fig. 2 plots a full revolution. The follower reaches its peak velocity of 1.214 m/s at θ = 49.5°, half way through the rise, when it has travelled 48.9 mm. Peak acceleration is 23.67 m/s^2 (2.41 g) at θ = 24.75° and 74.25°, accelerating the follower in the first half of the stroke and decelerating it in the second. Jerk stays finite, with a maximum of 923 m/s^3 at the ends of the stroke. The 180° return is much gentler, with a peak velocity of 0.668 m/s and a peak acceleration of 7.16 m/s^2. The asymmetry visible in Fig. 2 is what the cam is designed to produce.

TABLE IV. CYCLOIDAL FOLLOWER MOTION DURING THE 99° RISE

θ (°)	s_f (mm)	v_f (m/s)	v_h (m/s)	a_f (m/s^2)
0	0.00	0.000	0.000	0.00
11	0.86	0.142	0.145	15.21
22	6.40	0.502	0.511	23.31
33	19.12	0.910	0.928	20.50
44	38.14	1.177	1.200	8.09
55	59.66	1.177	1.200	−8.09
66	78.68	0.910	0.928	−20.50
77	91.40	0.502	0.511	−23.31
88	96.94	0.142	0.145	−15.21
99	97.80	0.000	0.000	0.00

Note: h = 97.8 mm, ω_c = 10.72 rad/s, β = 99°, v_h = 1.019 v_f.

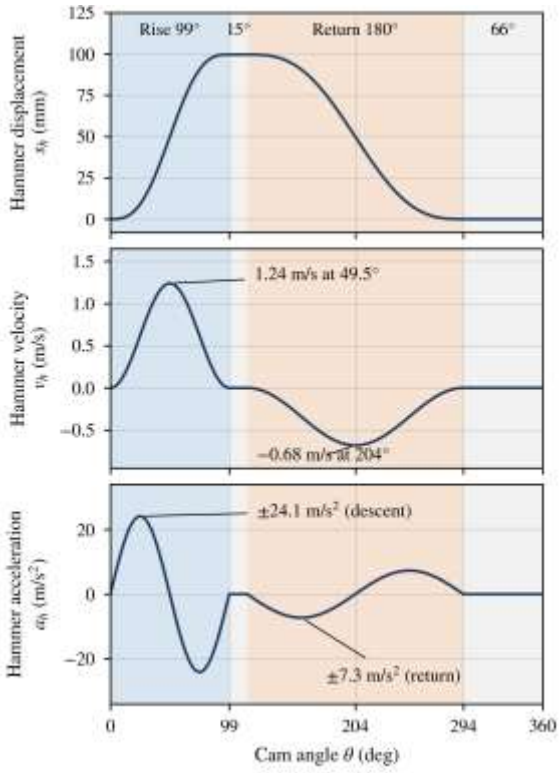


Fig. 2. Hammer displacement, velocity and acceleration over one cam revolution at 102.4 rpm. Follower values are scaled by i_L = 1.019 and downward is positive.

D. Hammer Velocity, Energy and Load

Through the lever ratio i_L = 1.019, the peak follower values become a peak hammer velocity of 1.237 m/s and a peak hammer acceleration of 24.1 m/s^2. The 2 kg hammer then carries E_k = 1.53 J at its fastest point, which lies 49.9 mm below its upper position. Its static weight is 19.6 N. At peak deceleration the lever must supply $F_{h,max}$ = 67.9 N, about 3.5 times the weight.

Table V compares the proposed motion with the two reference laws at the same stroke, shaft speed and mass and Fig. 3 shows the velocity histories. Shortening the descent from 180° to 99° raises peak velocity by a factor of 1.82 and kinetic energy by 3.31. Against simple harmonic motion the factors are 2.31 and 5.36. Peak acceleration rises by the same 3.31 relative to the symmetric cycloidal case (4.21 relative to simple harmonic), but because the hammer's weight does not change, the peak lever load rises by less: a factor of 1.98 (2.18).

TABLE V. MOTION LAWS COMPARED AT EQUAL STROKE, SPEED AND MASS

Motion law	Descent (°)	$v_{h,max}$ (m/s)	$a_{h,max}$ (m/s²)	E_k (J)	$F_{h,max}$ (N)
Simple harmonic (crank-like)	180	0.53	5.73	0.29	31.1
Cycloidal, symmetric	180	0.68	7.30	0.46	34.2
Cycloidal, proposed	99	1.24	24.13	1.53	67.9

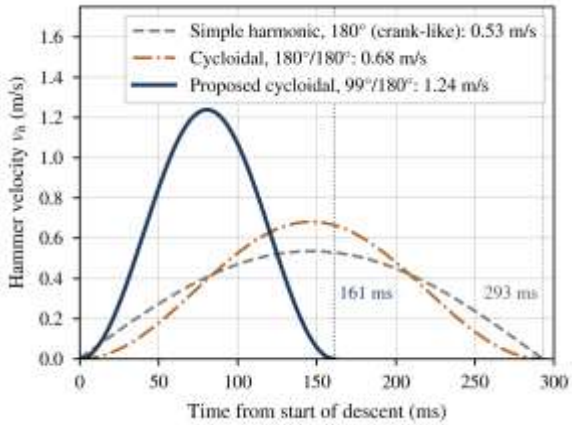


Fig. 3. Hammer velocity during the descent for three motion laws at the same stroke (99.7 mm) and shaft speed (102.4 rpm).

E. Sensitivity to Mass and Velocity

Table VI gives $E_k = \frac{1}{2}mv^2$ for masses and velocities around the design point. Doubling the velocity at constant mass quadruples the energy, whereas doubling the mass only doubles it: for the 2 kg hammer, raising the velocity from 0.75 to 1.50 m/s takes the energy from 0.56 J to 2.25 J. Reaching the proposed energy from the symmetric cycloidal case by adding mass instead would need a hammer of 6.6 kg (65 N static weight) and the peak lever load at the symmetric cycloidal acceleration would be 113 N, which is 1.67 times the 67.9 N of the proposed design.

TABLE VI. KINETIC ENERGY IN JOULES FOR DIFFERENT HAMMER MASSES AND VELOCITIES

m_h (kg)	0.75	1.00	1.237 (design)	1.50	1.75
1	0.28	0.50	0.77	1.12	1.53
2	0.56	1.00	1.53	2.25	3.06
3	0.84	1.50	2.30	3.38	4.59
4	1.12	2.00	3.06	4.50	6.12

Note: column headings are the hammer velocity v_h in m/s.

F. Effect of the Descent Angle

Because the 99° allocation is a design choice, Table VII repeats the calculation for other descent angles at the same stroke, shaft speed, hammer mass and cam size. Energy falls steadily as the angle widens, from 1.85 J at 90° to 0.46 J at 180° and the peak lever load falls with it. The pressure angle falls too. With the present 110 mm base circle and 15 mm roller it drops below 30° only for descent angles above about 115°, where the kinetic energy is 1.13 J, some 26% lower than at 99°. The 99° design therefore gets its extra energy by running past the pressure-angle limit.

TABLE VII. EFFECT OF THE DESCENT ANGLE ON HAMMER PERFORMANCE

Descent (°)	$v_{h,max}$ (m/s)	$a_{h,max}$ (m/s²)	E_k (J)	$F_{h,max}$ (N)	φ_{max} (°)
90	1.36	29.2	1.85	78.0	36.5
99	1.24	24.1	1.53	67.9	33.9
115*	1.06	17.8	1.13	55.1	30.0
150	0.82	10.5	0.67	40.6	24.0
180	0.68	7.3	0.46	34.2	20.3

Note: * pressure angle reaches 30° at 115.4°; 99° is the proposed design.

G. Power, Pressure Angle and Cost

Lifting the hammer through 99.7 mm takes 1.96 J per cycle or 3.34 W at 1.71 blows per second, which is 0.45% of the 746 W motor rating. The pressure angle peaks at 33.9° at $\theta = 43.7°$ during the rise and at 20.3° during the return. The cam has a 110 mm base circle, a maximum pitch-curve radius of about 223 mm and a thickness of 30 mm. Materials and fabrication for the prototype cost INR 13,040 (Table VIII).

TABLE VIII. MATERIAL AND FABRICATION COST OF THE PROTOTYPE

Item group	Contents	Cost (INR)
Drive motor	1 HP, 1440 rpm	4,000
Transmission	Pulleys, belts, pillow-block and ball bearings	4,180
Cam and lever parts	Cam, leaf spring, compression spring, fulcrum	2,060
Raw material	25 kg	1,600
Fasteners	50 pieces	500
Fabrication and finishing	Machining and paint	700
Total		**13,040**

5. DISCUSSION

A. What the Cam Angle Buys and Costs

Section IV shows one exchange in two currencies. Velocity scales as $1/\beta$ and acceleration as $1/\beta^2$, so shrinking the descent angle from 180° to 99° raises kinetic energy and peak acceleration by the same factor, $(180/99)^2 = 3.31$. Loads do not follow energy one for one, because the lever force $m_h(g + a_h)$ contains a term that does not depend on the motion law at all, the hammer's weight. For the 2 kg hammer, energy goes up by a factor of 3.3 while the peak lever load goes up by 2.0, so the descent angle is a cheap source of energy relative to the load it creates. It is not free. The same shortening lifts the pressure angle to about 34° and the compression spring must keep the roller on the cam through a peak acceleration of 2.41 g. The spring preload has not been calculated here. Table VII shows how the exchange plays out at other angles.

B. Velocity Versus Mass

The equivalent-energy comparison points the same way. Reaching 1.53 J by making the hammer heavier takes 6.6 kg, a static weight of 65 N and a 113 N peak load on the lever, link and bearings. Reaching it through the cam timing takes 2 kg and 67.9 N. Within this model, then, shaping the cam is the cheaper route to a given energy in terms of load, which is consistent with the aim of raising velocity and not mass.

C. How Far the Energy Figure Can Be Trusted

The 1.53 J figure is the kinetic energy at the instant of peak velocity not necessarily the energy delivered to the work. The cycloidal law brings the follower to rest at the end of the rise, so a hammer that stays in contact with the follower all the way down arrives at the bottom of its stroke with zero velocity. The full 1.53 J is available only if the work surface is set near mid-stroke, about 49.9 mm below the upper position or if the head is free to keep moving once the cam begins to slow it. Whether the compliant leaf-spring lever allows the second case can only be settled by measurement.

A second reference puts the numbers in perspective. A hammer simply dropped through 99.7 mm would reach 1.40 m/s and carry 1.96 J, more than the cam-driven peak of 1.24 m/s. The advantage claimed in this paper is therefore relative to a crank or a symmetric cam running at the same speed and it lies in a repeatable, motor-timed velocity profile. It is not a claim to beat gravity.

The pressure angle of 33.9° exceeds the 30° normally allowed for radial cams with translating roller followers [10]. Holding the same rise and timing within 30° would need a prime-circle radius of about 152 mm, which means a base circle of roughly 137 mm, some 25% larger than the 110 mm in the prototype. Separately, the 746 W motor rating is more than 200 times the 3.34 W needed to lift the hammer. The margin covers belt, bearing and spring losses and starting the drive, but it also means motor power was not what limited this design.

Finally, the model is ideal. It assumes rigid links, slip-free belts, a zero-offset follower and the CAD-derived lever ratio and it ignores friction and the elasticity of the leaf spring. Speed, vibration and impact energy have not been measured on the prototype.

D. Implications for Design

For designers of similar machines the practical message is to treat the descent angle as a variable and to read three quantities together: energy, which scales as β^{-2}; the peak lever load; and the pressure angle. Tables V, VI and VII give a quick way to do that for a given stroke and shaft speed. For this cam there are two ways to meet the 30° limit: widen the descent angle to about 115° and accept roughly 1.13 J or keep 99° and enlarge the base circle to about 137 mm. Either way, the spring preload and the follower guide would need to be sized for the resulting loads.

6. CONCLUSION

This paper worked a cam-driven mechanical hammer through from motor to hammer by calculation. A 1 HP, 1440 rpm motor and a three-stage V-belt reduction of 14.06:1 give a camshaft speed of 102.4 rpm, one blow every 0.586 s. A cycloidal cam that assigns 99° to the downstroke, 15° to a dwell, 180° to the return and 66° to a second dwell produces a peak hammer velocity of 1.24 m/s and 1.53 J of kinetic energy for a 2 kg hammer, with a peak acceleration of 24.1 m/s^2 and a peak lever load of 67.9 N. Compared with a symmetric cycloidal motion at the same stroke and speed, the energy is 3.3 times greater for a lever load 2.0 times greater and compared with simple harmonic motion it is 5.4 times greater. Reaching the same energy by adding mass would need a 6.6 kg hammer and a 113 N peak load. Materials and fabrication for the prototype cost INR 13,040.

The results come with limits that should be stated plainly. Nothing has been measured, so the energy, velocity and loads are ideal values from a rigid-body calculation. The 1.53 J is the kinetic energy at mid-stroke and is delivered in full only if the work surface is placed there or the hammer can separate from the lever. The cam-driven peak velocity is below that of a free drop through the same stroke, so the advantage is over symmetric drives at the same speed. The pressure angle of about 34° exceeds the usual 30° limit; with the present 110 mm base circle, meeting it would need a descent angle of about 115° and would cost roughly a quarter of the energy. The spring preload, the shaft and bearing sizes and the contact stress in the cam have not been calculated here.

Several steps would turn these calculations into tested results: instrumented measurement of hammer velocity and impact force on the prototype; a dynamic simulation of the cam, follower, lever and hammer that includes the compliance of the leaf spring; finite element checks of the frame, lever and shafts; a larger base circle or another adjustment to bring the pressure angle under 30°; and a comparison of other motion laws at the same 99° allocation. An adjustable stroke, speed control and guarding for the belts and cam would also be needed before any production use.

ACKNOWLEDGEMENT

The authors thank Prof. Utsav Dholakiya, Prof. Yogesh Dholariya (Head of Department), Dr. Virang Oza (Dean) of Mechanical Engineering, School of Engineering and Technology, Dr. Subhash University, Junagadh, for their guidance, co-operation and encouragement.

REFERENCES

[1] A. A. M. S. Al Aamri, S. Mudassir, M. V. Kulkarni, A. Hipolito and A. A. S. AlAwaid, “Modelling and fabrication of power hammer machine,” *EPRA Int. J. Multidiscip. Res.*, 2023.

[2] R. L. Norton, *Design of Machinery: An Introduction to the Synthesis and Analysis of Mechanisms and Machines*, 6th ed. New York, NY, USA: McGraw-Hill Education, 2020.

[3] M. J. Rider, *Design and Analysis of Mechanisms: A Planar Approach*. Hoboken, NJ, USA: Wiley, 2015.

[4] H. Qiu, C.-J. Lin, Z.-Y. Li, H. Ozaki, J. Wang and Y. Yue, “A universal optimal approach to cam curve design and its applications,” *Mech. Mach. Theory*, vol. 40, no. 6, pp. 669–692, 2005.

[5] T. T. N. Nguyen, S. Kurtenbach, M. Hüsing and B. Corves, “A general framework for motion design of the follower in cam mechanisms by using non-uniform rational B-spline,” *Mech. Mach. Theory*, vol. 137, pp. 374–385, 2019.

[6] M. Mandal and T. K. Naskar, “Introduction of control points in splines for synthesis of optimized cam motion program,” *Mech. Mach. Theory*, vol. 44, no. 1, pp. 255–271, 2009.

[7] G. Gatti and D. Mundo, “On the direct control of follower vibrations in cam–follower mechanisms,” *Mech. Mach. Theory*, vol. 45, no. 1, pp. 23–35, 2010.

[8] H. D. Desai and V. K. Patel, “Computer aided kinematic and dynamic analysis of cam and follower,” in *Proc. World Congr. Eng. (WCE)*, vol. II, London, U.K., 2010, pp. 1246–1250.

[9] L.-I. Wu, W.-T. Chang and C.-H. Liu, “The design of varying-velocity translating cam mechanisms,” *Mech. Mach. Theory*, vol. 42, pp. 352–364, 2007.

[10] A. H. de Freitas Avelar and L. F. Soares, “Nomograms for maximum pressure angles in radial cams with follower eccentricity for cycloidal and harmonic motion curves,”

Acta Sci. Technol., vol. 45, e57823, 2023, doi: 10.4025/actascitechnol.v45i1.57823.
[11] R. S. Khurmi and J. K. Gupta, *A Textbook of Machine Design*. New Delhi, India: S. Chand Publishing, 2019.
[12] R. Perneder and I. Osborne, *Handbook Timing Belts: Principles, Calculations, Applications*. Berlin, Germany: Springer, 2012.
[13] F. Pellicano, G. Catellani and A. Fregolent, "Parametric instability of belts: theory and experiments," *Comput. Struct.*, vol. 82, no. 1, pp. 81–91, 2004.
[14] G. Čepon and M. Boltežar, "Dynamics of a belt-drive system using a linear complementarity problem for the belt–pulley contact description," *J. Sound Vib.*, vol. 319, no. 3–5, pp. 1019–1035, 2009.
[15] S. Chowdhury and R. K. Yedavalli, "Dynamics of belt–pulley–shaft systems," *Mech. Mach. Theory*, vol. 98, pp. 199–215, 2016.
[16] L. Bertini, L. Carmignani and F. Frendo, "Analytical model for the power losses in rubber V-belt continuously variable transmission (CVT)," *Mech. Mach. Theory*, vol. 78, pp. 289–306, 2014.